ANCIENT PALEO-ERG DEPOSITS IN APOLLINARIS SULCI – A RECORD OF AEOLIAN SYSTEM CHANGE AND PRESERVATION.

M. Chojnacki[1], M. Jodhpurkar[2], L. K. Fenton[3], L. A. Edgar[2], C. Edwards[4], A. R Weintraub[4]. [1]Planetary Science Institute, Tucson, AZ (mchojnacki@psi.edu); [2]USGS, Astrogeology Science Center, Flagstaff, AZ. [3]Carl Sagan Center, SETI Institute, Mountain View, CA.[4]Northern Arizona University, Flagstaff, AZ.

Introduction and Motivation: Wind driven sand dunes and smaller bedforms are scattered across the surface of Mars today. These aeolian landforms are also found throughout the geologic record and attest to the enduring presence of wind as one of the dominant geologic agents (*1*). Where identified, these geologic units may preserve clues about past environmental and climate conditions. For example, rover investigations have firmly established that some of the ~4 Ga rock record is composed of sediment transported by flowing wind and water, as evidenced by abundant cross-bedding and fine layering (*2*, *3*).

One of the initial reports documenting ancient aeolian dunes came from analysis of Mars Global Surveyor MOC images of Apollinaris Sulci deposits (*4*). That study described a field of moderate albedo, crescent-shaped features with superposed craters that were proposed to be ancient duneforms. Here we revisit that location with new data, analysis, and revelations about other "paleo-bedform" sites on Mars (*5*, *6*).

Outstanding questions related to the nature of ancient bedform formation and modification history include: What are the circumstances by which these features are preserved? What geologic periods do paleo-bedforms appear to be associated with? What does local and regional paleo-bedform morphology imply about paleo-flow regimes?

Data Sets and Methods: We assessed aeolian deposits using five adjacent Digital Terrain Models (DTMs) (at 1 m post spacing) and orthoimages (0.25–1 m/pix) (**Fig. 1**) acquired by the High Resolution Imaging Science Experiment (HiRISE) (*7*). DTMs were controlled to a Context Camera (CTX) DTM and Mars Orbiter Laser Altimeter (MOLA) data for absolute elevation. HiRISE slope maps at ~3-5 m baselines were derived from DTMs using a 3x3 low pass filter on the terrain. Additional insight of paleo-bedform thermophysical trends was obtained using THEMIS data (*8*).

Results: *Context* – The study site is found on the southeast flank of Apollinaris Sulci (northeast of Gusev crater) (178°E, 12°S). The area is bracketed by a highly dissected Amazonian-Hesperian undivided unit (Ahtu) to the north and a smoother Middle Noachian highland unit (mNh) to the south (**Fig. 1**) (*9*). The 33-km-wide deposit covers an area of 140 km^2, which is comparable to numerous moderate scale modern dune fields (*10*).

Morphology – Mapping reveals several distinct clusters of broadly crescentic, positive-relief features that resemble barchan and barchanoid dunes in the center of the deposits, and barchan- and/or transverse-like landforms on the margins of the deposit. Some units display elongated limbs which appear to merge or bifurcate in areas – common characteristics for bedforms. Meter-scale stratification is evident on the steeper (lee) faces and is suggestive of cross-bedding.

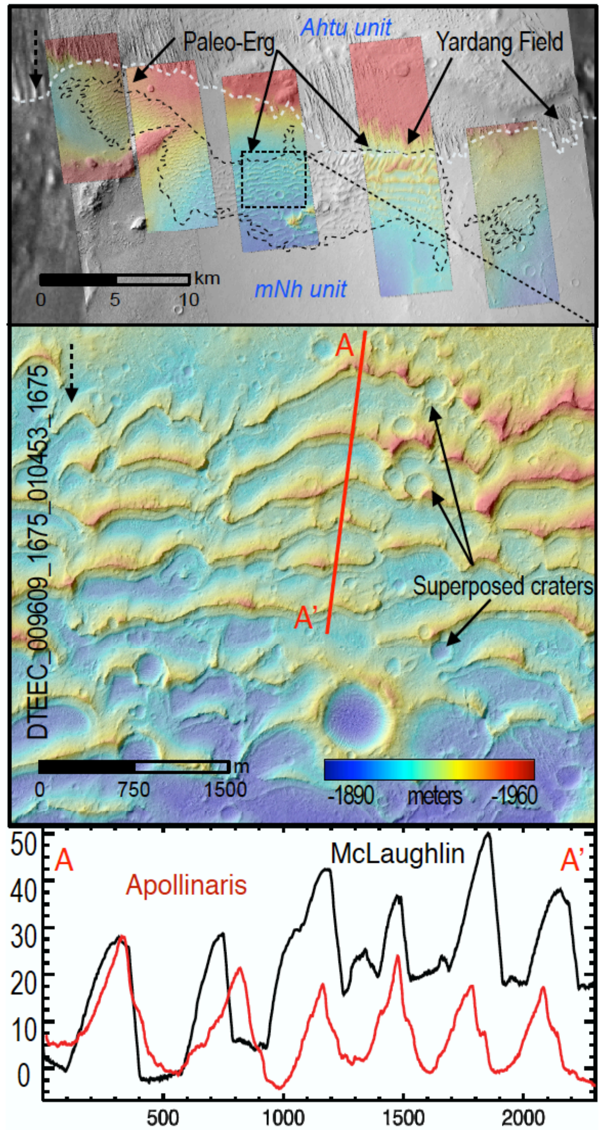

Figure 1. (top) Context view of Apollinaris Sulci paleo-erg (black polygon), yardang field (green line) and the HiRISE DTM coverage. (middle) Color altimetry overlaid on an orthoimage showing paleo-dune topography. (bottom) Relief (m) profiles of Apollinaris paleo (red) vs. McLaughlin crater modern (black) dunes, revealing similar height-to-wavelength relationships.

Whereas most of these landforms are 8-35 m tall (**Fig. 2**) some exceed 100 m in relief. As their height increases so does their spacing (300-750 m). These parameters along with their length (200-900 m) and width (300-2000 m) are similar to many modern martian and terrestrial aeolian dunes (*10*) (**Fig. 2**). Given the spatial distribution, consistent orientation, and geometric parameters, these landforms are interpreted to be lithified aeolian sand dunes.

Preservation – The Apollinaris duneforms display superposed craters, boulders, fractures, and abundance of dust mantles or smaller bedforms. Impact crater size ranges from 50-600 m in diameter (**Fig. 1**). This size range and their distribution may indicate these are mostly primary impacts rather than secondary, which may allow relative ages to be extracted. Thermal inertia of these deposits is very low (145+/–37 $Jm^{-2}K^{-1}s^{-1/2}$), likely indicating an unconsolidated dusty surface which is not representative of the primary paleo-dune surfaces.

Slope analysis reveals a regular asymmetric trend to the paleo-dunes. What are identified as stoss slopes are consistently flatter (~5-12°) than the south-facing lee slopes (~15-30°) (**Fig. 3**). Remarkably, some of the best preserved lee-sides exceed 30° and are at or above the static angle of repose. This indicates a strong cementing agent has lithified the sand component as these steep slopes would be most susceptible to mass-wasting. This level of preservation is uncommon on Earth where lee-dune faces may be fully eroded.

In comparison to contemporary McLaughlin dunes, Apollinaris paleo-dunes are similar or taller at a given spacing (**Fig. 2**). We also compared these with previously identified paleo-dunes in Melas Chasma (**Fig. 2**)(*6*) which are 2-3× smaller in relief and more eroded,

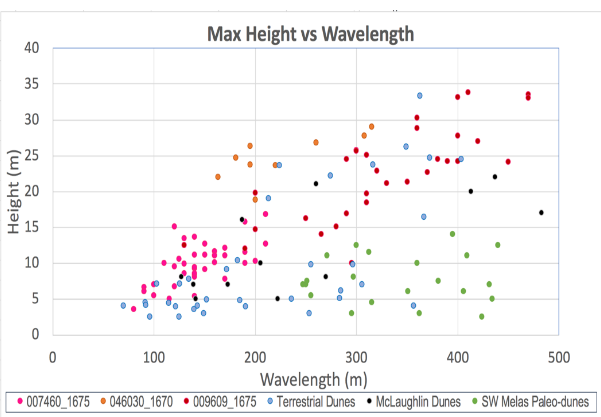

Figure 2. Log-log plot of height vs. wavelength for Apollinaris paleo (magenta, orange, red) and modern dune fields. Contemporary terrestrial (blue) (*11*) and McLaughlin crater dunes are also plotted. Note the tighter and steeper trends for Apollinaris paleo-dunes compared with Melas paleo-dunes coverage.

perhaps suggesting a greater sediment supply (when active) and/or greater preservation for Apollinaris paleo-dunes. In contrast, several of the eastern most paleo-barchans are eroded down to their bases, indicating a range of preservation states across the erg.

Wind regime – The lee faces only deviate ~50° in azimuth from due south indicating a northerly wind regime was responsible for most central paleo-dune morphologies, with northeasterly and northwesterly variations more apparent on the flanks. We also note the massive yardang field to the north (**Fig. 1**) was carved by quasi-northerly (toward ~165°) winds (broadly perpendicular to lee-faces), indicating a formidable and relatively consistent wind regime perhaps spanning different geologic epochs.

Geologic history – The transitional undivided unit (Ahtu) to the north comes into contact with paleo-erg in central locations. As inferred earlier from lower resolution data (*4*), the yardang field appears to be stratigraphically above the erg as viewed in HiRISE suggesting the unit is older and is being removed by erosion. Based on various lines of evidence the yardang-forming unit (similar to the Medusae Fossae Formation) has been interpreted to be a pyroclastic deposit (*9*), perhaps sourced by Apollinaris Mons and responsible for the paleo-erg preservation. Future efforts will seek to better constrain the geologic history of Apollinaris Sulci paleo-erg.

Conclusion: Results confirm that Apollinaris Sulci records an ancient aeolian dune field. The dune field contained both transverse and barchanoid dunes, with comparable bedform properties to modern aeolian dunes, that migrated broadly to the south with variations on flanks (consistent with superimposed yardangs). Comparison to previously reported paleo-dunes in Melas Chasma suggests that paleo-bedforms are a common feature on Mars, spanning different geologic settings and potentially different ages.

Acknowledgments: This research was supported by NASA MDAP Grant NNH16ZDA001N and the MRO/HiRISE mission. We would like to thank UArizona/HiRISE staff for assistance with targeting and Christine Akers for DTM production.

References: [1] Grotzinger J. & R. Milliken (2012) *Sed. geo. of Mars*. [2] Edgar L. & J. Grotzinger (2012) *Sed. geo. of Mars*. [3] Banham S. et al. (2018) *Sediment.* sed.12469. [4] Edgett K. & M. Malin (2000) *JGR-Plan. 105*, 1623–1650. [5] Durrant L. et al. (2017) *Planet. Space Sci.* 148, 45–55. [6] Chojnacki M. et al. (2019) *GSA Meet.* Abs #337776. [7] McEwen et al. (2007) *JGR* 112, 2005JE002605. [8] Weintraub A. et al. (2020) *LPS LI,* Abstract #3053. [9] Tanaka K. et al. (2014) *Planet. Space Sci.* 95, 11–24. [10] Hayward, R. (2014) *Icarus*, *230,* 38–46. [11] Lancaster, N (1988) *Geology, 16,* 972.